

새로운 Vane 혼합기로 제조된 Polypropylene과 Halloysite 나노튜브의 나노복합재료

Xiaochun Yin, Sai Li, Liang Wang, Guangjian He[†], and Zhitao Yang

The Key Laboratory of Polymer Processing Engineering of Ministry of Education, South China University of Technology
(2016년 6월 30일 접수, 2016년 8월 22일 수정, 2016년 10월 11일 채택)

Nanocomposites of Polypropylene and Halloysite Nanotubes Prepared by a Novel Vane Mixer: Morphology, Thermal, Mechanical and Rheological Properties

Xiaochun Yin, Sai Li, Liang Wang, Guangjian He[†], and Zhitao Yang

The Key Laboratory of Polymer Processing Engineering of Ministry of Education, South China University of Technology,
Guangzhou, 510640, China

(Received June 30, 2016; Revised August 22, 2016; Accepted October 11, 2016)

Abstract: Halloysite nanotubes (HNTs) were used to prepare polypropylene (PP) nanocomposites through a novel vane mixer. The effects of melt blend time and halloysite content on properties of composites were investigated. SEM analysis was performed to show that HNTs were well dispersed in PP matrix with the increase of mixing time. DSC showed both the degree of crystallinity and crystallization temperature increased due to the introduction of HNTs into PP, which indicating a potential nucleation effect induced by the nanotubes. TGA illustrated that the presence of HNTs had two opposite effects on the thermal behavior. A surface catalytic action of the halloysite speeded up thermal degradation of PP. However, this effect was reduced with improved HNTs dispersion. Rheological investigations revealed that rheological properties were significantly increased by the addition of low fraction of halloysite to PP. The 2 wt% HNTs nanocomposites reached maximum tensile strength because HNTs dispersed evenly in PP.

Keywords: nanocomposites, halloysite nanotubes, mixing, polypropylene.

Introduction

The incorporation of nanofillers into a polymer matrix to prepare nanocomposites has received extensive attention in the last two decades, due to the overwhelming properties of these nanocomposites compared to conventional polymer composites. The physical properties of these nanocomposites, such as electric insulativity, thermomechanical performance and wearing resistance, could be dramatically improved by even adding a small amount of nanofillers.¹⁻⁴ The commonly used nanofillers include carbon nanotubes, montmorillonite, kaolin, calcium carbonate, halloysite and so on,^{5,6} and their nanocomposites are applied in a wide range of field, including automotive, home appliances, and construction.^{7,8}

Among all these nanofillers, HNTs ($\text{Al}_2[\text{Si}_2\text{O}_5(\text{OH})_4]\cdot 2\text{H}_2\text{O}$)

combines similar chemical properties as montmorillonite and geometrical appearance as carbon nanotubes, which is rich in nature resources and less expensive. It mainly consists of hollow tubes with length up to 2 μm and outer diameter in the range of 30-50 nm,⁹ which reveals a high aspect ratio and surface energy. Compared with other clay silicates, HNTs can be more easily dispersed in a polymer matrix due to the weak secondary interactions among the nanotubes via hydrogen bonds and van der Waals forces.¹⁰

Polypropylene (PP) is one of the most popular commodity polymers, which has well-balanced physical and mechanical properties as well as good processability. HNTs as a promising nanofillers were also used to reinforce PP, which were usually compounded through twin-screw extruder, and the properties of HNTs/PP were reported in several works. Prashantha *et al.*¹¹ studied the influence of the addition of both unmodified HNTs and quaternary ammonium salt modified HNTs (QM-HNTs) on structural and mechanical properties of PP nanocomposites. Their result showed that QM-HNTs were well dispersed in PP

[†]To whom correspondence should be addressed.
E-mail: hegj@scut.edu.cn

©2017 The Polymer Society of Korea. All rights reserved.

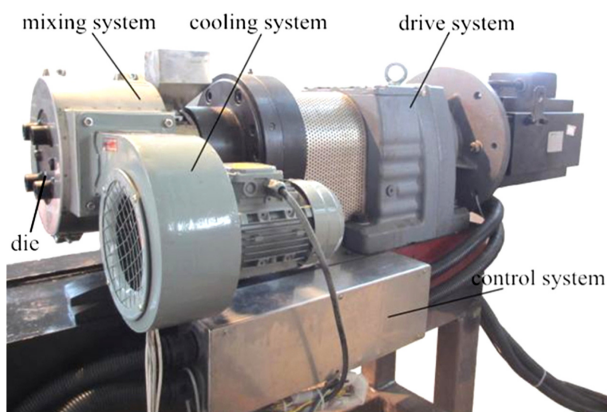


Figure 2. Picture of the vane mixer.

were then extruded out through the outlet die, and granulated after air cooling to room temperature. The pellets were directly used for thermogravimetric analysis (TGA) or differential scanning calorimetry (DSC) testing after being dried for 4 h. In addition, the pellets were compression molded into sheets with a thickness of 1 or 4 mm by a compression molding machine (QBL-350, Wuxi No. 1 Rubber & Plastics Mechanical Co. Ltd, China) at 200 °C and 10 MPa for 6 min. The 1 mm sheets were used for rheology and mechanical testing, and the 4 mm sheets were used for morphological characterization.

Scanning Electron Microscope (SEM). Samples for morphological investigations of the nanocomposites were prepared by fracturing the 4 mm thick molded sheets in liquid nitrogen. The fracture surface of specimens was sputter coated with a thin gold layer to avoid charging during SEM imaging. Then the morphology was investigated using a scanning electron microscope that was equipped with a field emission cathode (LEO 1530 VP, Zeiss, Germany). The acceleration voltage was varied and ranged between 0.1 and 30 kV.

Thermo-gravimetric Analysis (TGA). The thermal stability of pure PP and the nanocomposites were studied by thermo-

gravimetric analysis (TGA). The analysis were performed using a TG 209 F3 Tarsus (NETZSCH, Germany). Solid samples weighed about 4 mg and they were heated from room temperature to 600 °C at a heating rate of 10 °C/min under nitrogen atmosphere with a flow rate of 100 mL/min.

Differential Scanning Calorimetry (DSC). The different scanning calorimetry (DSC) was used to study the thermal properties of the composites. A DSC 204 F1 Phoenix (NETZSCH, Germany) was used at a heating/cooling rate of 10 °C/min in the temperature range 30-200 °C for determination of the thermal transitions. A heating-cooling-heating cycle was applied to eliminate the thermal history of the samples. Each sample had a net weight about 4-6 mg. According to the record DSC thermograms, crystallization temperature (T_c), melting temperature (T_m), heat of fusion (ΔH_m) and relative degree of crystallization (X_c) were determined. X_c was calculated from the DSC crystallization curves with eq. (1):

$$X_c = \frac{\Delta H_m}{\Delta H_m^0(1-\omega_f)} \quad (1)$$

where ΔH_m is the particular heat of fusion or melting heat, calculated by integrating the area under the crystallization peak, ΔH_m^0 is the theoretical specific melting heat of 100% crystalline isotactic PP, which is taken as 209 J/g,²¹ and ω_f is the weight fraction of fillers.

Melt Rheology. The rheological properties of neat PP and the nanocomposites were investigated by using a Physica MCR302 rheometer (Anton Paar, Austria). The melt flow properties at low shear rates and small deformations were examined by liner viscoelastic shear oscillations. The measurement temperature was 200 °C. The diameter of cylindrical samples was 25 mm and their thickness was 1 mm. The melting time of sample was set up 5 min. The measurements of samples were performed in a nitrogen atmosphere in case the degradation of PP.

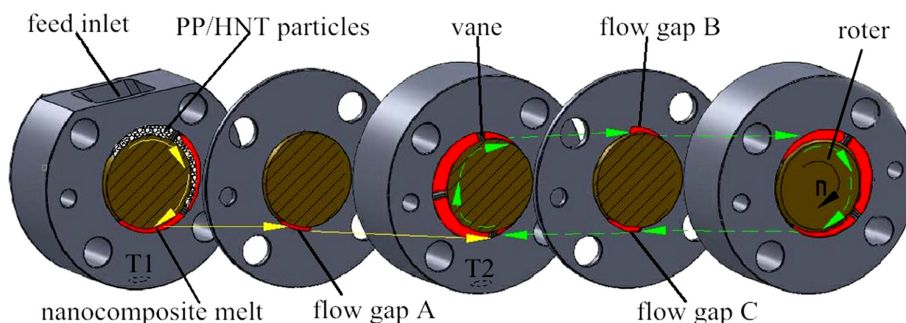


Figure 3. Mixing schematic of the vane mixer.

Mechanical Testing. In order to investigate the tensile strength of the PP/HNTs nanocomposites standard dumbbell specimens (according to GB/T 1040-1992) with dimensions of 75×20×4 mm were cut from 1 mm thick molded sheets. All specimens were tested by using ETM 104B (Wance, China) with a crosshead velocity of 5 mm/min. Five specimens were tested for each sample and the average values were reported.

Results and Discussion

Morphology. Figure 4 showed the SEM morphology of the as received powder of the mineral halloysite. As can be seen, raw HNTs present the state of aggregation. It is difficult to determine the primary size of HNTs precisely because of aggregate nature of the nanotubes and large size distribution of halloysite. The diameter ranges from 30 to 50 nm and the length/diameter ratio is the range of 10-40. Clearly, HNTs has the similar geometry as the multi wall carbon (MWCNTs), but in comparison to CNTs, HNTs has the advantage of being less stick to the matrix, which makes them easier to be dispersed in the viscous polymer matrix.²²

The effects of mixing time on the morphology of PP/HNTs nanocomposites with 6 wt% HNTs are presented in Figure 5. From Figure 5(a) to 5(d), it can be seen that HNTs micro-particles existed in PP matrix. However, the size of HNTs particles reduced immensely with the increase of mixing time. As shown in Figure 5(a) to 5(d), the mean of the area of circled HNTs particles were about 2.09×10^{-2} , 3.43×10^{-3} , 2.47×10^{-4} , 1.01×10^{-4} mm², respectively. Compared to the nanocomposites mixed for 1.5 or 3 min, the size of HNTs particles in the nanocomposite mixed for 4.5 min reduced sharply. But the HNTs

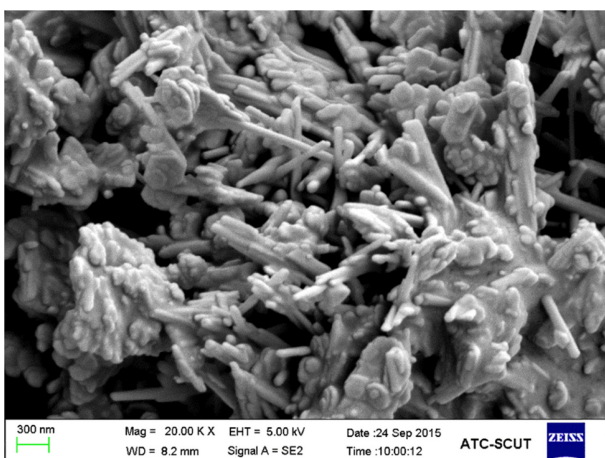


Figure 4. SEM micrograph of raw HNTs.

particles size was not further reduced when mixing time was further increased to 6 min. As can be seen from the higher magnification micrographs (Figure 5(e) to 5(h)), some aggregations of HNTs were observed when the mixing time was 1.5 or 3 min from Figure 5(e) and 5(f). However, the HNTs were dispersed individually in PP matrix without any indication of aggregation were observed on the whole investigated area when the mixing time was 4.5 or 6 min. This indicated that the HNTs were dispersed more homogenously in PP matrix with the increase of mixing time. This phenomenon can be explained that the nanocomposite melt in extensional flow field experienced more cycles of stress due to the increased mixing time, which allows enough stress to break up aggregations of HNTs and results more uniform distribution.

Furthermore, some small cavities presented on the fracture surface for all the nanocomposites can be observed, indicating that part of the nanotubes did not break during cold fracture but can be pulled out of the PP matrix (Figure 5(e) to 5(h)). Similar phenomenon was also reported in previous work,²³ suggesting weak interfacial interaction between HNTs and the PP matrix.

Thermal Properties. The effects of HNTs content on the thermal stabilities of the PP/HNTs nanocomposites are presented in Figure 6. As shown in Figure 6, the weight loss of PP and composites was one step. For all the nanocomposites, the temperature at 5 wt% weight loss ($T_{5\%}$) increased compared to pristine PP. The $T_{5\%}$ increased approximately 10 °C when the HNTs concentration increased from 2 to 6 wt%. However, the $T_{5\%}$ increased only 3 °C when the HNTs concentration is 8 wt%. This phenomenon may be concluded that low HNTs content has a better HNTs dispersion which was also reflected by rheology. Additionally, aggregation may increase with the increase of HNTs concentration due to high surface energy of HNTs. As reported, the degradation of PP in nitrogen is initiated primarily by the random thermal scissions of C-C chain bonds and the intermolecular transfer of hydrogen. For HNTs with hollow tubular structure, it could be concluded that the lumen of HNTs is the main effect on improving the thermal stability of PP/HNTs composites at the initial degradation stage. This can be ascribed that the degradation products of PP may fairly be entrapped into the lumen of HNT, which leading to effective delay in mass transport. Such phenomenon was also reported by Du *et al.*¹³ HNTs in the polymer can protect weight loss in the early stage ($T_{5\%}$), consequently, halloysite nanotubes may also be adequate fillers for high temperature thermoplastic.

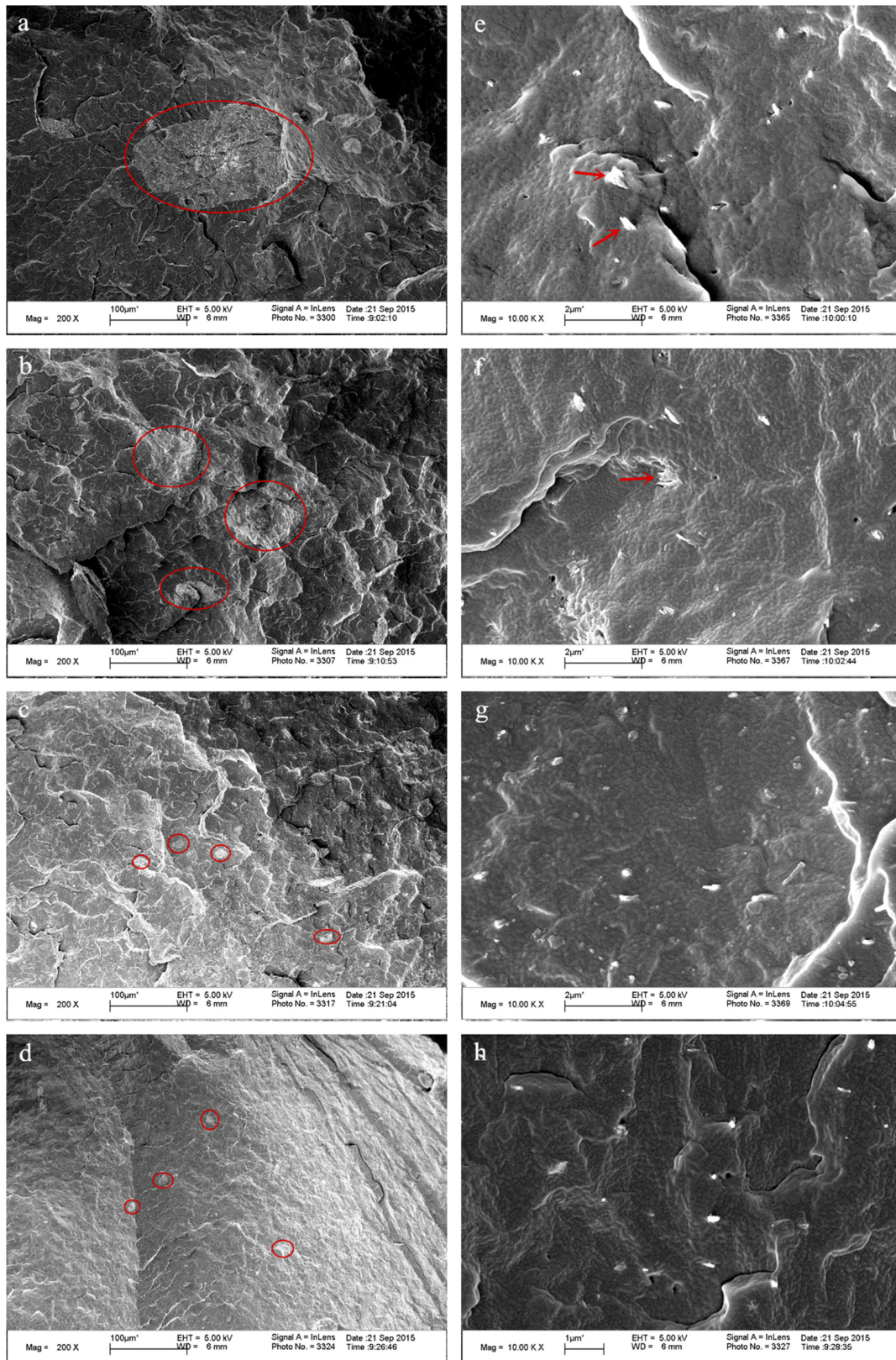


Figure 5. SEM micrographs of PP/HNTs nanocomposites at different mixing time with low and high magnification: (a,e) 1.5 min; (b,f) 3 min; (c,g) 4.5 min; (d,h) 6 min.

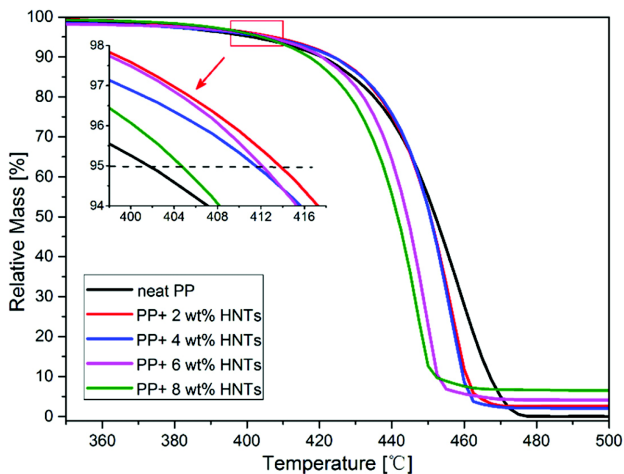


Figure 6. TGA analysis of the pure PP and nanocomposites (mixing time, 3 min).

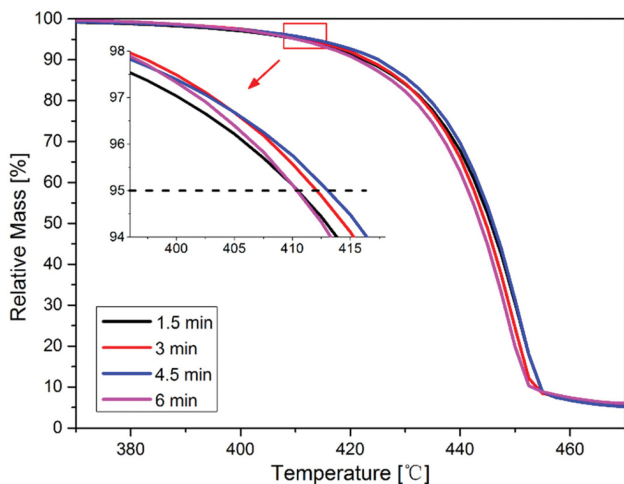


Figure 7. TGA analysis of the nanocomposites of different mixing time (HNTs content, 6 wt%).

It is also worth noticing that HNTs presents a catalytic action on PP pyrolysis as a result of the existence of hydroxyl groups (Al-OH) that via Brönsted acid sites acting in catalysis. The catalytic effect of clay nanoparticles on thermal degradation of polymer has already been demonstrated by Tartaglione.²⁴ The catalytic effect of HNTs was more obviously in PP/HNTs nanocomposites with higher HNTs content. That could also be the reason why $T_{50\%}$ of 8 wt% HNTs nanocomposites is lower than these 2 to 6 wt% PP/HNTs composites and the degradation speed of nanocomposites were faster than pure PP in the lately stage.

The effect of mixing time on the thermal stabilities of the PP/HNTs composites is presented in Figure 7. As shown in

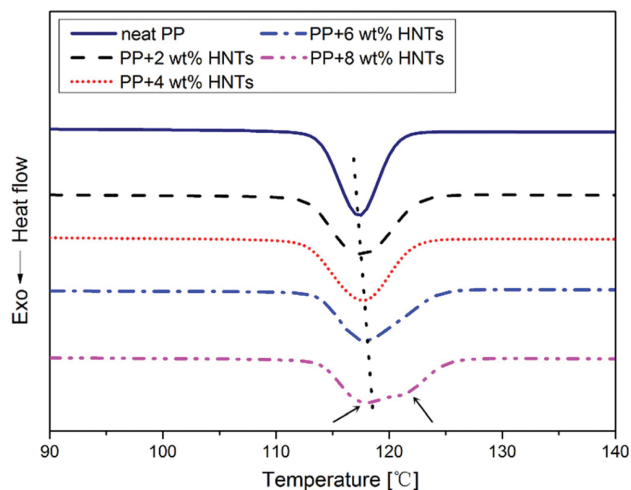


Figure 8. DSC cooling thermograms of PP and nanocomposites of different HNTs content (mixing time, 3 min).

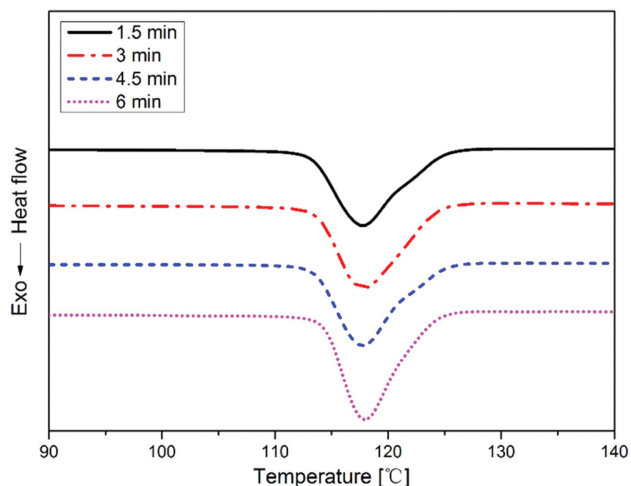


Figure 9. DSC cooling thermograms of PP and 6 wt% HNTs nanocomposites at different mixing time.

Figure 7, the thermal stability of PP/HNTs nanocomposites was slightly improved with a better HNTs dispersion by increasing the mixing time. However, the presence of nanoclay and long time high local extensional/shear stress may also lead to a thermal-mechanical degradation on PP.¹² Thus, it was the reason for the deviation for the curve which mixed 6 min.

Figure 8 and 9 showed the crystallization curves obtained during cooling of the PP/HNTs nanocomposites at different HNTs loadings and mixing time, respectively. Relative degree of crystallinity (X_c), crystallization temperature (T_c), melting temperature (T_m) and heat of fusion (ΔH_m) of various nanocomposites (second heating run) were reported in Table 1 and Table 2. As shown in Figure 8 and Table 1, the crys-

Table 1. T_c , T_m , ΔH_m and X_c Values for PP and Nanocomposites at Mixing 3 min

Samples	T_c (°C)	T_m (°C)	ΔH_m (J/g)	X_c (%)
Neat PP	117.3	161.7	78.45	37.5
PP+2wt% HNT	117.5	163.0	84.63	41.3
PP+4wt% HNT	117.7	164.0	79.21	39.5
PP+6wt% HNT	117.8	162.4	80.51	41.0
PP+8wt% HNT	118.0	162.5	78.22	40.7

Table 2. T_c , T_m , ΔH_m and X_c Values for 6 wt% HNTs Nanocomposites at Different Mixing Time

Mixing time (min)	T_c (°C)	T_m (°C)	ΔH_m (J/g)	X_c (%)
1.5	117.7	162.9	77.05	39.2
3	117.8	162.4	80.51	41.0
4.5	117.7	162.5	80.92	41.2
6	117.9	161.1	88.09	44.8

tallization behavior of PP was affected by the addition of HNTs. All crystallinity (X_c) of the nanocomposites were increased compared to pristine PP. Meanwhile, both the T_c and T_m of PP slightly shifted to higher temperature. These results further indicate that halloysites may act as nucleation sites for the crystallization of PP matrix and accelerate the growth rate of spherulite.²⁵ The maximum increase in percentage crystallinity was observed for 2 wt% HNTs filled nanocomposite. This may be ascribed to the fact that the dispersion of halloysites becomes more evenly at relatively lower HNTs content, resulting higher efficiency in enhancing the crystallinity. Moreover, the DSC cooling thermograms of composite with 8 wt% HNTs in Figure 8 appeared two crystalline peak, that means HNTs dispersed in PP were not uniform, which may be caused the crystallization of PP was not perfect.

As shown in Figure 9 and Table 2, the mixing time also affected the crystallization behavior of PP. No significant change was observed in the T_c and T_m of nanocomposites, but with the increase of mixing time, X_c of the composites increased significantly. This suggested that dispersion of HNTs was improved with increasing mixing time, resulting increased efficiency in heterogeneous nucleation effect.

Rheological Properties. Rheological characterization is usually used as an indirect measurement to estimate the dispersion state of the filler in polymer matrix. Indeed, rheological behavior at high frequencies is used to evaluate the effect of the filler on processing properties, and the complex viscosity to steady shear viscosity can break down the normal

Cox-Merz rule in complex systems like composites. Low frequency behavior is sensitive to the structure, the size and the shape of the dispersed phase. The storage modulus (G') and the complex viscosity (η^*) increase in the low frequency regime may be associated to interfacial interactions between polymer chains and filler surface and/or with better dispersion of the filler in polymer matrix.²⁶ Furthermore, the formation of a percolated filler network structure in polymer matrix is usually presented by existing a plateau for G' at low frequencies accompanied with a continuous increase of η^* .^{27,28}

The storage modulus of PP/HNTs nanocomposites as a function of frequency is presented in Figure 10(a). According to the linear viscoelastic theory, it is generally believed that the G' of polymer based composites increase monotonously with an increase of the frequency. From Figure 10(a), it can be seen that the theory was compatible in this work as the G' of pure PP and the PP/HNTs nanocomposites increased with the increase of frequency. It also can be observed from Figure 10(a) that all composites showed a higher of G' than pure PP when the frequency was no more than 0.3 rad/s. However, a differentiation of G' was observed when the frequency is above 1 rad/s. The storage modulus of the 2 and 4 wt% HNTs nanocomposites were still higher than pure PP. But for the 6 and 8 wt% HNTs nanocomposites, the storage modulus were lower than pure PP. The results indicated that a better dispersion of HNTs in PP can lead to higher G' . A similar phenomenon was found by Lecouvet *et al.*¹² in investigating the effect of water-assisted extruded PP/HNTs composites.

The complex viscosity of pure PP and PP/HNTs nanocomposites as a function of frequency was shown in Figure 10(b). It can be seen that the PP/HNTs composites (2 and 4 wt% HNTs) had a similar dependence on frequency as pure PP. Both of the composites and pure PP showed the characteristic of a Newtonian fluid in that η^* kept almost constant when the frequency was less than 1 rad/s. Compared to pure PP, the η^* of PP/HNTs nanocomposites (2 and 4 wt% HNTs) increased significantly. Increased η^* for PP/HNTs composites is a common phenomenon for filler reinforced polymer materials. It was a better nanotubes dispersion contributed to improve the interaction between the HNTs and PP which hindering the movement of the PP chains. Similar phenomenon was reported for nano-CaCO₃ filled PBS composite by Chen.²⁹

However, a strong shear thinning effect and nearly linear viscosity curve were observed for the composites (6 and 8 wt% HNTs) within whole investigated frequency range. And the η^* of PP/HNTs composites (6 and 8 wt% HNTs) were lower than

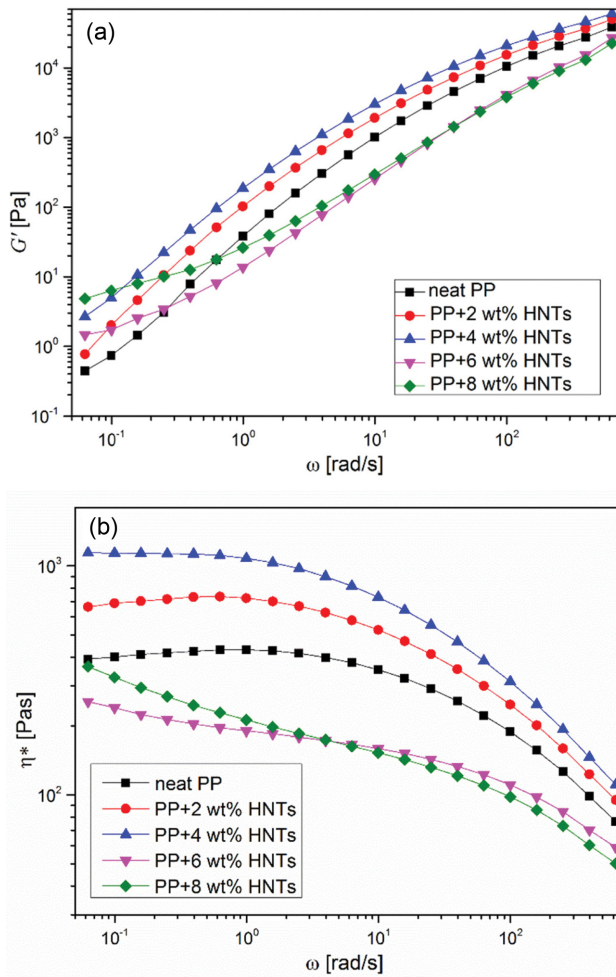


Figure 10. (a) Storage modulus (G'); (b) complex viscosity (η^*) of pure PP and nanocomposites (mixing time, 3 min).

pure PP. The strong shear thinning phenomenon indicated the filler dominated fluid in the nanocomposites with a relatively high HNTs loading. The transition in η^* indicated that the nanocomposites have reached a rheological percolation.^{30,31} Moreover, a thermo-mechanical degradation occurring during melt processing due to higher local stress applied by HNTs on PP chains resulted in the average molecular weight decrease.^{12,32} Thus, the decrease of complex viscosity in comparison with pure PP may be explained by poor HNTs dispersion in PP matrix and lower molecular weight in the composite.³³ Rheological measurements were in perfect agreement with the TG or DSC results that the relatively low content HNTs had a better dispersion in PP matrix. Actually, in this paper, the percolated network structure formed starting from 6 wt% HNTs, the transition from a liquid-like to a solid-like behavior was visible in rheological measurements by the trend of a plateau

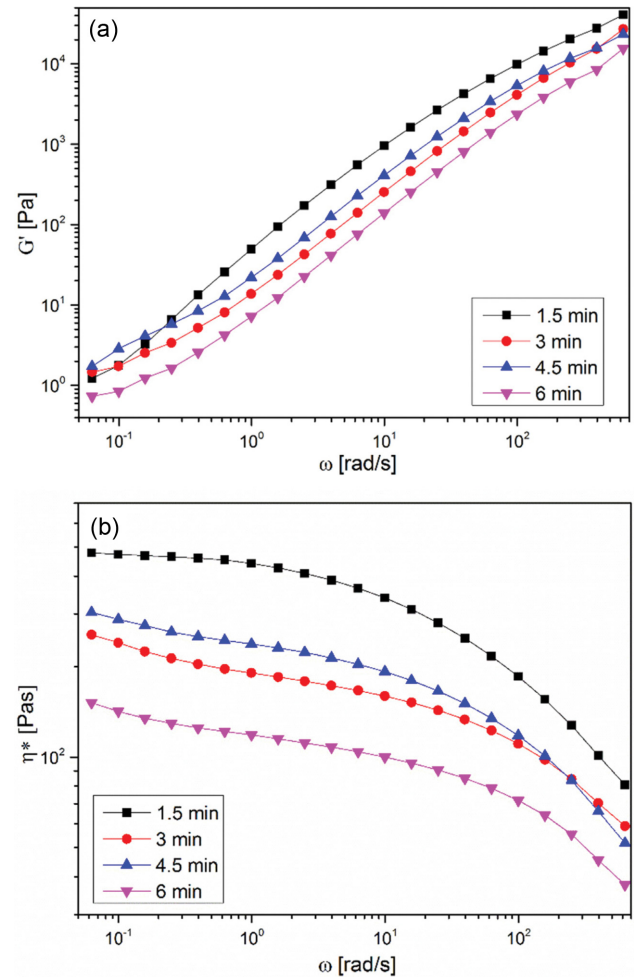


Figure 11. (a) Storage modulus (G'); (b) complex viscosity (η^*) of 6 wt% HNTs nanocomposites at different mixing time.

for storage modulus at low frequencies combined with a continuous rise of complex viscosity (Figure 10). As the nanotube content increases in composite system, nanotube-nanotube interactions begin to dominate, eventually lead to percolation and the formation of an interconnected structure of nanotubes.³⁴

Figure 11(a) and 11(b) showed the effect of mixing time on viscoelastic properties of nanocomposites. As the mixing time increased, the storage modulus and the complex viscosity decreased in most frequency regime. This phenomenon can be explained as following: (i) the molecular chains of PP are liable to orientate under the extensional/shear flow, (ii) the presence of high content nanoclay and high local extensional/shear stress lead to a thermal-mechanical degradation of PP result in the average molecular weight decrease.^{12,32} Moreover, due to the nanocomposite melt in extensional flow field experienced

more cycles of stress as the mixing time increased, this may result in the reduction of aspect ratio of the halloysite nanotubes, which caused the drop in G' and η^* of composites. Considering two factors (i and ii) and the better dispersion of the nanofiller in polymer matrix contribute to increase η^* , which caused the G' and η^* of composite (mixed for 3 min) was lower than those of composite (mixed for 4.5 min), but was higher than those of the composite (mixed for 6 min). These results indicated three mechanisms were in competition. And the factor (i) was compatible with the DSC results that the more mixing time led to the higher crystallinity (X_c) of nanocomposites.

Tensile Properties. The effects of both HNTs content and mixing time on the tensile strength of pure PP and composites were presented in Figure 12. It could be found that mixing time had a little influence on the tensile strength of the neat PP and composites. However, the maximum tensile strength reached 37 MPa when the HNTs content is 2 wt%, which increased 15% compared to neat PP. This mainly because the HNTs can disperse evenly in PP matrix and have strong interaction when the HNTs dispersed well in PP matrix. This effect will be favorable for stress transfer at the interface when external forces are exerted on the composites. And the pulling out of HNTs from PP matrix during tensile stretching can release tensile stress and delay the break down of the samples,³⁵ the cavities of pulling out of HNTs in PP matrix can be observed from SEM micrographs. Moreover, the composites containing 2 wt% HNTs had the biggest increment on crystallinity, the maximum increase of crystallinity was responsible for the improvement in tensile strength.³⁶ The tensile strength of the

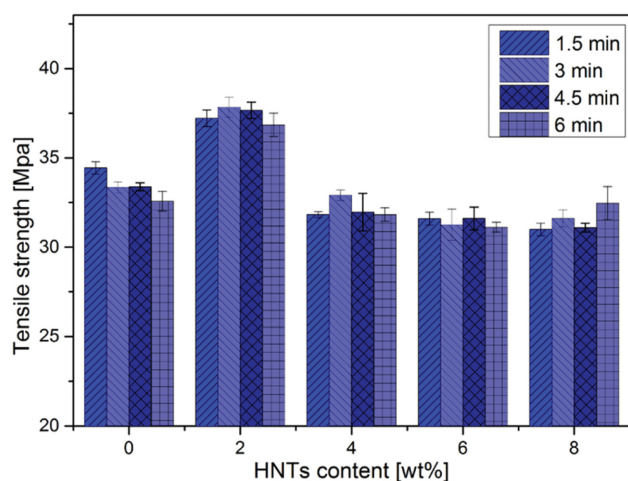


Figure 12. Tensile strength of pure PP and nanocomposites (error bars represent standard deviation).

composites with 4, 6 or 8 wt% HNTs decreased slightly compared with neat PP, this may be caused by the HNTs aggregations in PP matrix, which resulted in lots of big voids appearing at lower tensile stress and subsequent a premature yielding.^{10,37} And a poor HNTs dispersion in PP matrix resulting in stress concentration which caused the decrease of the composites tensile strength.

Conclusions

In this work, PP/HNTs nanocomposites have been prepared by a novel vane mixer. Effects of HNTs concentration and mixing time on properties of the nanocomposites were analyzed. (a) The morphological characterization revealed that HNTs dispersed uniformly in PP matrix within 6 min. The size of HNTs particles in the nanocomposites mixed for 4.5 min reduced sharply compared to the nanocomposites mixed for 1.5 and 3 min, which leveled off with further increase in mixing time. (b) The TGA results confirmed that the incorporation of HNTs enhanced the thermal stability of PP/HNTs nanocomposites compared to pure PP due to the lumen of HNTs. Furthermore, appropriate mixing time can slightly improve the thermal stability of the composites. (c) The DSC results indicated that the HNTs had the obviously nucleating effect, the crystallinity of the composites increased and the melting peak shifted to higher temperature with the increase of HNTs content. Additionally, the addition of 2 wt% HNTs led to maximum crystallinity on PP due to a better HNTs dispersion. The crystallinity of composites increased more than 5% as the mixing time increased. (d) The rheological measurements showed that the storage modulus and complex viscosity of composites decreased with the increase of mixing time. And the 2 and 4 wt% HNTs nanocomposites performed the higher storage modulus and complex viscosity compared to neat PP.

Acknowledgments: The authors are thankful for the financial support from National Natural Science Foundation of China (Grant No. 51435005 and 51403068), the Natural Science Foundation of Guangdong Province (2016A030313004), and the Fundamental Research Funds for the Central Universities (Project numbers 2015ZZ067 and 2015ZZ132).

References

1. P. Kiliaris and C. D. Papaspyrides, *Prog. Polym. Sci.*, **35**, 902 (2010).

2. H. S. Ryu, Y. S. Lee, J. C. Lee, and K. Ha, *Polym. Korea*, **37**, 308 (2013).
3. S. Pavlidou and C. D. Papaspyrides, *Prog. Polym. Sci.*, **33**, 1119 (2008).
4. H. G. Kim, *Polym. Korea*, **40**, 9 (2016).
5. R. Davand and M. Frounchi, *Polym. Korea*, **40**, 232 (2016).
6. M. Alexandre and P. Dubois, *Mat. Sci. Eng. R*, **28**, 1 (2000).
7. M. Guessoum, S. Nekkaa, F. Fenouillot-Rimlinger, and N. Haddaoui, *Int. J. Polym. Sci.*, **2012**, 1 (2012).
8. M. G. Juan, J. M. David, B. Jozef, F. Richard, and G. M. David, *Adv. Mater.*, **12**, 1835 (2000).
9. M. Du, B. Guo, and D. Jia, *Polym. Int.*, **59**, 574 (2010).
10. M. Du, B. Guo, X. Cai, Z. Jia, M. Liu, and D. Jia, *e-Polymers*, **8**, 1490 (2008).
11. K. Prashantha, M. F. Lacrampe, and P. Krawczak, *Express. Polym. Lett.*, **5**, 295 (2011).
12. B. Lecouvet, M. Sclavons, S. Bourbigot, J. Devaux, and C. Bailly, *Polymer*, **52**, 4284 (2011).
13. M. Du, B. Guo, and D. Jia, *Eur. Polym. J.*, **42**, 1362 (2006).
14. U. A. Handge, K. Hedicke-Höchstötter, and V. Altstädt, *Polymer*, **51**, 2690 (2010).
15. D. C. O. Mamey, L. J. Russell, D. Y. Wu, T. Nguyen, D. Cramm, N. Rigopoulos, and M. Greaves, *Polym. Degrad. Stabil.*, **93**, 1971 (2008).
16. H. Ismail, P. Pasbakhsh, M. N. A. Fauzi, and A. A. Bakar, *Polym. Test.*, **27**, 841 (2008).
17. Z. Jia, Y. Luo, B. Guo, B. Yang, M. Du, and D. Jia, *Polym.-Plast. Technol.*, **48**, 607 (2009).
18. C. Rauwendaal, *Plast. Addit. Compd.*, **10**, 32 (2008).
19. J. P. Qu, H. Z. Chen, S. R. Liu, B. Tan, M. L. Liu, X. C. Yin, Q. J. Liu, and R. B. Guo, *J. Appl. Polym. Sci.*, **128**, 3576 (2013).
20. X. Yin, Z. Yu, G. He, Z. Yao, and B. Xu, *J. Appl. Polym. Sci.*, **132**, 41551 (2015).
21. H. G. Kim, *Polym. Korea*, **40**, 9 (2016).
22. Y. Ye, H. Chen, J. Wu, and L. Ye, *Polymer*, **48**, 6426 (2007).
23. B. Lecouvet, J. G. Gutierrez, M. Sclavons, and C. Bailly, *Polym. Degrad. Stabil.*, **96**, 226 (2011).
24. G. Tartaglione, D. Tabuani, G. Camino, and M. Moisio, *Compos. Sci. Technol.*, **68**, 451 (2008).
25. M. Du, B. Guo, J. Wan, Q. Zou, and D. Jia, *J. Polym. Res.*, **17**, 109 (2009).
26. A. V. Shenoy, *Rheology of filled polymer systems*, Springer Science & Business Media B. V., p. 243 (2013).
27. P. Pötschke, T. D. Fornes, and D. R. Paul, *Polymer*, **43**, 3247 (2002).
28. A. J. Hsieh, P. Moy, F. L. Beyer, P. Madison, E. Napadensky, J. Ren, and R. Krishnamoorti, *Polym. Eng. Sci.*, **44**, 825 (2004).
29. R. Chen, W. Zou, H. Zhang, G. Zhang, Z. Yang, G. Jin, and J. Qu, *Polym. Test*, **42**, 160 (2015).
30. Q. Wang, X. Zhang, C. J. Wang, J. Zhu, Z. Guo, and D. J. O'Hare, *Mater. Chem.*, **22**, 19113 (2012).
31. J. Zhu, S. Wei, Y. Li, L. Sun, and N. Haldolaarachchige, *Macromolecules*, **44**, 4382 (2011).
32. J. Y. Nam, S. S. Ray, and M. Okamoto, *Macromolecules*, **36**, 7126 (2003).
33. Q. Li, Q. Zeng, Y. Huang, Y. Lv, Q. Li, and Q. Yang, *J. Mater. Sci.*, **48**, 948 (2013).
34. S. S. Ray, K. Okamoto, and M. Okamoto, *Macromolecules*, **36**, 2355 (2003).
35. B. Li, F.-X. Dong, X.-L. Wang, J. Yang, D.-Y. Wang, and Y.-Z. Wang, *Eur. Polym. J.*, **45**, 2996 (2009).
36. L. C. Arruda, M. Magaton, R. E. S. Bretas, and M. M. Ueki, *Polym. Test.*, **43**, 27 (2015).
37. S. Zhao, S. Qiu, Y. Zheng, L. Cheng, and Y. Guo, *Mater. Design*, **32**, 957 (2011).